Positron Annihilation Studies of Chromophore-Doped Polymers

Chia-Ming Huang, Eckard W. Hellmuth, and Y. C. Jean*

Department of Chemistry, University of Missouri−Kansas City, Kansas City, Missouri 64110

Received: November 17, 1997; In Final Form: February 10, 1998

Positron annihilation lifetime experiments have been performed in two chromophores, Disperse Red 1 (DR1) and Disperse Orange 3 (DO3), doped in a poly(methyl methacrylate) polymer (PMMA) as a function of temperature. Significant chemical quenching and inhibition effects on positronium annihilation due to doping are observed. These effects are interpreted in terms of a chemical reaction between positronium and chromophore molecules and a change of free volume and hole properties in polymers. Diffusion coefficients of positronium in polymers are found to be on the order of 10^{-6} cm^2/s and to increase with temperature. The activation energy for the reaction between positronium and chromophores is found to be 4 and 8 ± 1 for DO3 and 10 and 15 ± 1 kJ/mol for DR1, at the glassy and the rubbery states, respectively. Both orthopositronium lifetime and differential scanning calorimetry analyses show that doping polymers results in a significant decrease to glass transition temperature. Applications of positron annihilation spectroscopy to study the effect of free volume and holes in nonlinear optical polymeric materials are discussed.

I. Introduction

In recent years, there has been an increasing interest in the study of nonlinear optical (NLO) properties of organic polymeric materials because of their technological importance.[1] Organic polymeric materials have major advantages for development as an NLO material, including an intrinsically low dielectric constant, flexible molecular design, and ease of processing.[2]

An NLO polymeric system basically is composed of two major components: the polymer matrix and the chromophore. A chromophore is typically a polarizable molecule consisting of one or several electron donors and electron acceptors covalently bound to a π-conjugated segment to form a molecular dipole. Chromophores can be either doped into or cross-linked to the polymer matrix to form NLO polymers.[3] To form an NLO material, the chromophore-doped polymers are poled along the direction of an applied electric field. Corona poling and contact poling are two common techniques used to orient chromophores in NLO polymers.[4]

The second harmonic generation (SHG) measurement is often used to determine the optical properties of NLO polymeric systems.[4−6] Amorphous polymers doped with NLO chromophores have been shown to exhibit a SHG property.[4,6] Polymer mobility and relaxation phenomena provide an ideal host environment for doped NLO chromophores to align in preferred orientations.[6,7] Although the performance of NLO polymers is comparable with traditional inorganic crystals, the SHG signal always decays with increasing time and temperature.[8] Signal decay is attributable to the chromophore disorientation in the polymer matrix; this eventually eliminates the noncentrosymmetric property which is required for the application of NLO devices. Previous studies show that the doping of small molecules is confirmed by the free volume theory.[9,10] Polymer chain segmental motions in polymer-based NLO systems are thought to be directly related to the local free volume and hole properties around the dopants.[11]

Positron annihilation lifetime (PAL) spectroscopy has been developed in the past decade and proven to be a novel probe to study the free volume and hole properties of polymeric systems.[12−19] In this work, we report the initial results of a positron annihilation study on two commonly known chromophore/polymer systems.

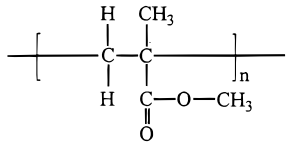

Poly (methyl methacrylate) (PMMA)

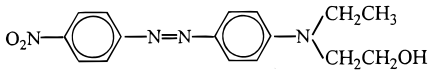

Disperse Red 1 (DR1)

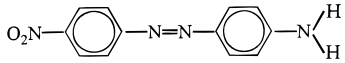

Disperse Orange 3 (DO3)

Figure 1. Chemical structures of polymer and doping chromophores in this study.

II. Experiments

1. Sample Preparations. Figure 1 shows the chemical structure of the polymer and two commercially available dyes used in this study. Poly(methyl methacrylate) (PMMA), having an average molecular weight of 120 000 and density of 1.187 g/cm^3, was purchased from Aldrich Chemical Co., Milwaukee, WI. Disperse Red 1 (DR1) and Disperse Orange 3 (DO3) were also purchased from Aldrich Chemical Co. Acetone (reagent grade) was used as the solvent to prepare chromophores at a weight fraction of 1%, 2%, and 3% (w/w) in PMMA. Different concentrations of doped PMMA samples having a thickness of ca. 1−2 mm were prepared using the standard solvent casting

S1089-5647(98)00231-4 CCC: $15.00
Published on Web 03/17/1998

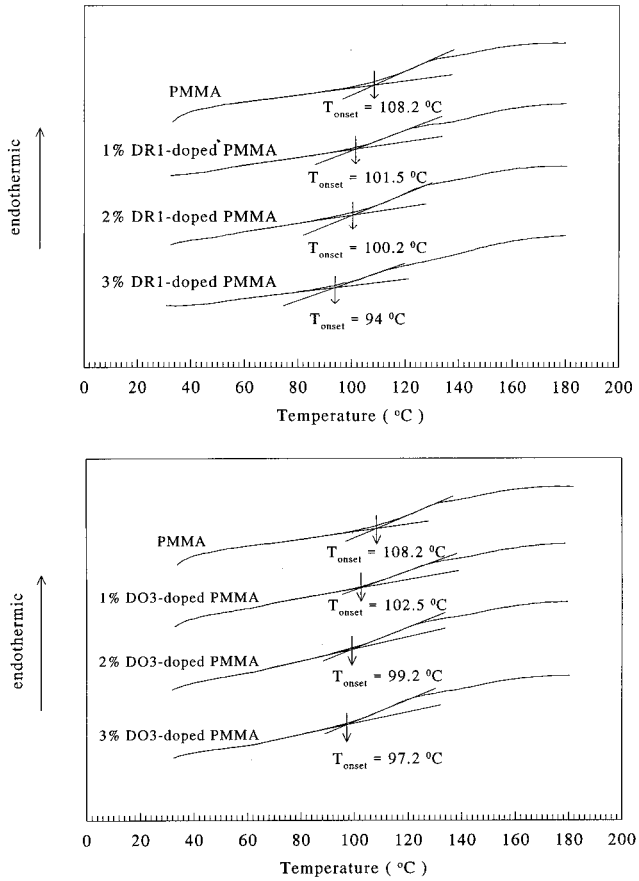

Figure 2. DSC curves for DR1/PMMA and DO3/PMMA systems.

method on glass plates. The prepared chromophore-doped PMMA samples were dried under vacuum at an elevated temperature (80 °C) for at least 6 h to completely remove the solvent before the PAL experiments.

2. DSC Measurements. A differential scanning calorimeter (DSC, Polymer Labs. model 3) was used to monitor the heat flow of prepared chromophore/polymer samples as a function of temperature. The glass transition temperature, T_g, of PMMA was determined to be 108.2 °C by DSC with a heating rate of 10 °C/min. The DSC analysis of all doped samples was also carried out using the same heating rate. The DSC plots for the samples used in this positron study are shown in Figure 2. The melting points, determined by DSC analysis, of DR1 and DO3 are 160 and 200 °C, respectively.

3. Positron Annihilation Lifetime Measurements. The positron annihilation lifetimes (PAL) were determined by detecting the prompt γ-ray (1.28 MeV) from the nuclear decay that accompanies the emission of a positron from the ^{22}Na radioisotope and the annihilation γ-rays (0.511 MeV). All PAL spectra were recorded using the fast−fast coincidence circuit of a PAL spectrometer with a lifetime resolution of about 260 ps, monitored using a ^{60}Co source. Many spectra (between 1 $\times$ 10^6 and 20 $\times$ 10^6 counts) were collected on each sample for a complete data analysis—both a discrete lifetime and a distribution. The counting rate was approximately 120 counts/s. Detailed descriptions of PAL can be found elsewhere.[20] PAL experiments were performed as a function of temperature in different weight fractions of chromophores in PMMA polymers.

All PAL spectra obtained were analyzed employing the PATFIT program,[21] which decomposes a PAL spectrum into two to five terms of negative exponential, and the CONTIN program,[22] which gives a lifetime distribution. Another computer program, MELT,[23] was used to confirm the consistency of the results analyzed by both methods.[24] In these chromophore/polymers, we found that three-lifetime results give the best χ^2 (<1.1) and most reasonable standard deviation. The shortest lifetime ($\tau_1 \approx 0.12$ ns) is that of p-Ps (singlet Ps); the intermediate lifetime ($\tau_2 \approx 0.40$ ns) is the lifetime of the unbound positron. The longest lifetime ($\tau_3 \approx 1-3$ ns) is due to o-Ps annihilation. Since τ_1 does not vary with temperature or concentration, we have fixed $\tau_1 = 0.125$ ns in the final data analysis.

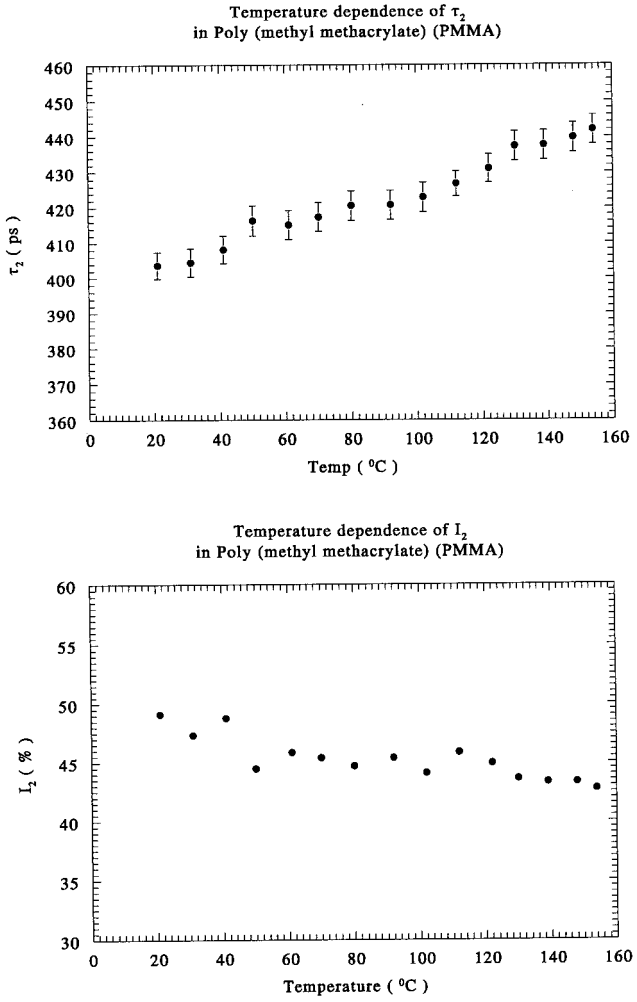

Figure 3. Intermediate positron lifetime (τ_2) and intensity vs temperature of pure PMMA.

In the current PAL method, we employ the results of the o-Ps lifetime distribution (τ_3) to obtain the mean free-volume hole radius (R) by the following semiempirical equation:[25−27]

$$\tau_3 = \frac{1}{\lambda_3} = \frac{1}{2}\left[1 - \frac{R}{R_0} + \frac{1}{2\pi}\sin\left(\frac{2\pi R}{R_0}\right)\right]^{-1} \qquad (1)$$

where τ_3 and R are expressed in nanoseconds and angstroms, respectively. R_0 equals $R + \Delta R$, where ΔR is the fitted empirical electron layer thickness (=1.66 Å).

The fractional free volume, F_v (%), is expressed as an empirically fitted equation:[28]

$$F_v = AV_fI_3 \qquad (2)$$

where V_f (in Å^3) is the hole volume calculated using the spherical radius (R) of eq 1 from τ_3, I_3 (in %) is its intensity,

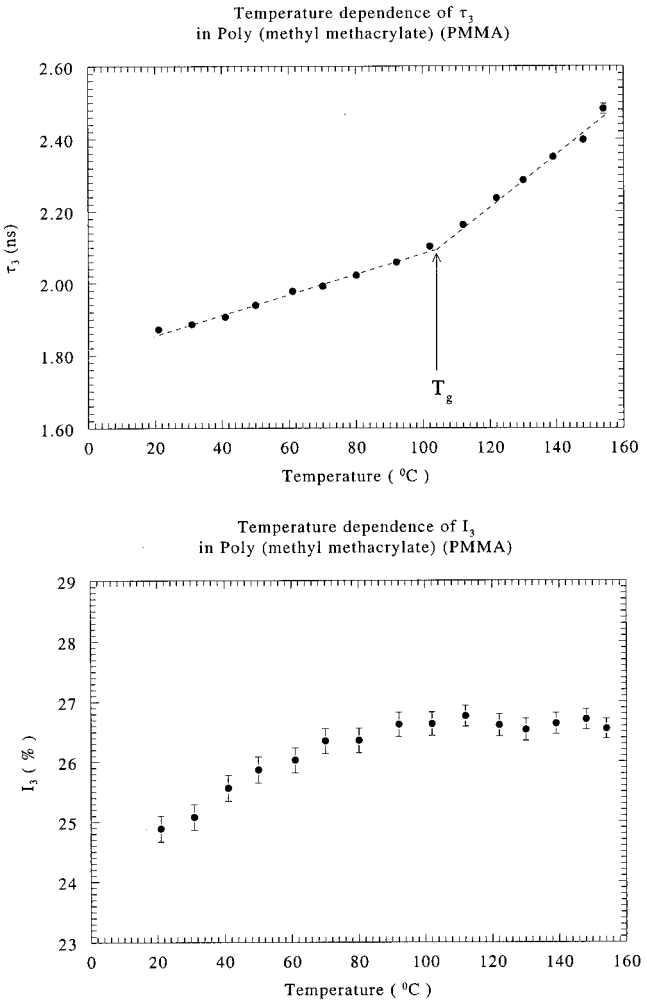

Figure 4. o-Ps lifetimes (τ_3) and intensities (I_3) vs temperature of pure PMMA.

and A is empirically determined to be 0.0018 from the specific volume data.[28]

III. Results and Discussion

1. Free Volume Hole Size and Fraction in PMMA. PAL results in PMMA have been reported by several groups.[29−31] In Figures 3 and 4, we plot the τ_2 (unbound positron lifetime), I_2 (corresponding positron intensity), τ_3 (o-Ps lifetime), and I_3 (corresponding o-Ps intensity) vs temperature, as obtained from POSITRONFIT analysis in the PATFIT package. These are consistent with the reported data: lifetimes increase with temperature as a result of hole size expansion. Since polymers are very complicated systems and our PAL results may vary slightly from samples chosen by others, we wish to present detailed PAL data from the current PMMA for a clear comparison with doped samples. The onset temperature of τ_3 was used to identify T_g as 104 °C, which is slightly lower than the DSC result (108 °C). The increased τ_2 vs temperature also indicates the localization of the positrons in free volumes and holes of polymers. The increased I_3 in the glassy state is interesting and consistent with the published results.[29,31] It appears that most thermosets, such as epoxies,[32,33] show an increased I_3 in the rubbery state (above T_g), while thermoplastics such as polycarbonates,[34,35] polystyrene,[13] and PMMA show a large temperature dependence in the glassy state (below T_g). Hole radii (R) and volumes are then calculated according to eq 1 in a spherical hole model and are shown in Figure 5. The

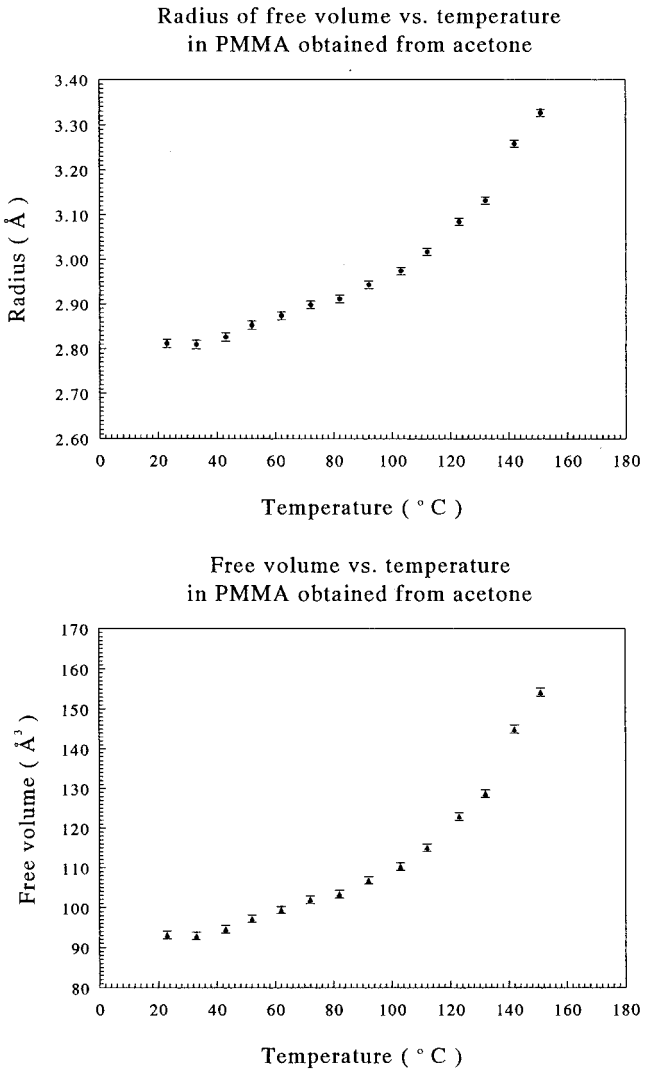

Figure 5. Hole radius and volume in pure PMMA vs temperature.

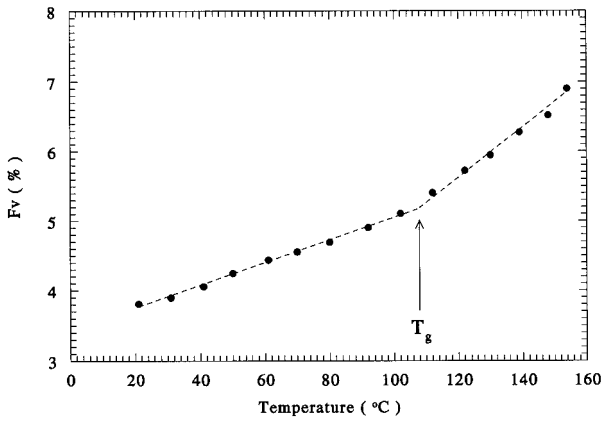

Figure 6. Free volume fraction (F_v) in pure PMMA vs temperature.

fractional hole volume is calculated from eq 2 and is plotted vs temperature in Figure 6. The onset temperature from the F_v plot (108 °C) is closer to the DSC result than that from the o-Ps data (τ_3 of Figure 4). This indicates that it may be better to compare the T_g obtained from other conventional methods, such as DSC, with those from F_v, rather than from τ_3.

The distribution of hole radii of PMMA at different temperatures is calculated from the result of o-Ps distribution resolved from the CONTIN program using the method described elsewhere.[36] The radius distribution ranges from 2 to 4 Å and

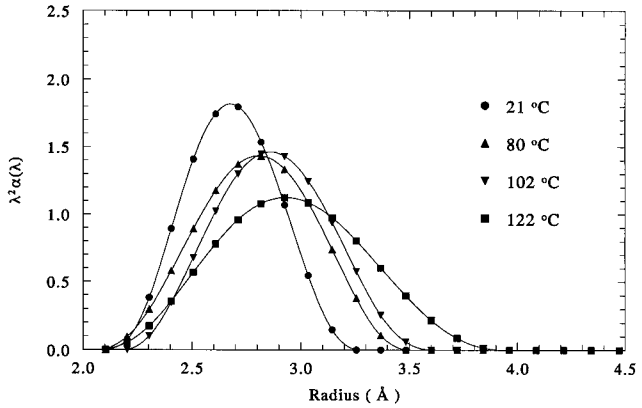

Figure 7. Hole radius distribution in pure PMMA at different temperatures.

is plotted in Figure 7. The kinetic radius of the chromophores is estimated to be 4.76 and 4.50 Å for DR1 and DO3, respectively, according to the reaction data for Ps and (3.3 Å) nitrobenzene.[37] Comparing these radii with the hole radii of PMMA shown in Figure 7, it can be seen that the chromophore molecules are too large to fill the existing holes in PMMA before doping.

2. Annealing Effects. We have performed PAL experiments in these solvent-cast samples as a function of annealing temperature. Each sample was annealed during the data acquisition time, which took about 3 h for each temperature. The experiments were performed from room temperature to about 160 °C, which is more than 50 °C above T_g. Variations of I_3 and τ_3 are shown in Figures 8−11 for DR1 and DO3 doped PMMA samples. These results show a large change as a function of annealing temperature and cycling. As shown in Figures 8 and 10, o-Ps lifetime (τ_3) and positron lifetime (τ_2) during the first run (incompletely annealed) are longer than in PMMA. A longer lifetime indicates that Ps quenching is insignificant for unannealed doped samples, and at the same time, that doping creates larger defects in the samples.

The temperature where the largest change of lifetime occurs coincides with T_g of doped polymers. During the first run and below the glass transition, the chromophore molecules are presumed to be nonuniformly dispersed and coagulated into a large cluster in the polymer matrix. The nonuniformly dispersed chromophores have effectively created larger defects in the polymer. Increased lifetime below T_g is indicative of expansion of free volume and holes as a function of temperature. However, when the temperature is above T_g, the polymer segments gain sufficient mobility to allow the chromophore molecules to move and segregate into single molecules in the polymer. A uniformly dispersed chromophore molecule above T_g then reacts chemically with Ps, causing the so-called "quenching" of Ps. The quenching effect shortens the o-Ps lifetime, as observed in Figures 8 and 10 where τ_3 decreases when T is higher than T_g.

During the second run (Figures 8 and 10), τ_3 increases as a function of temperature comparable to the undoped PMMA results (Figure 4) but starts with a shorter lifetime at room temperature. The onset temperature of τ_3 vs temperature also coincides with T_g as shown in Figures 8 and 10. The variation of intensity, I_3, with respect to temperature is less sensitive than lifetime, as shown in Figures 9 and 11. After the second run, we proceed to perform a third run of temperature dependence experiments. The PAL results of the third run reproduce those of the second run, thus indicating that the doped systems are uniformly dispersed after the first run experiments.

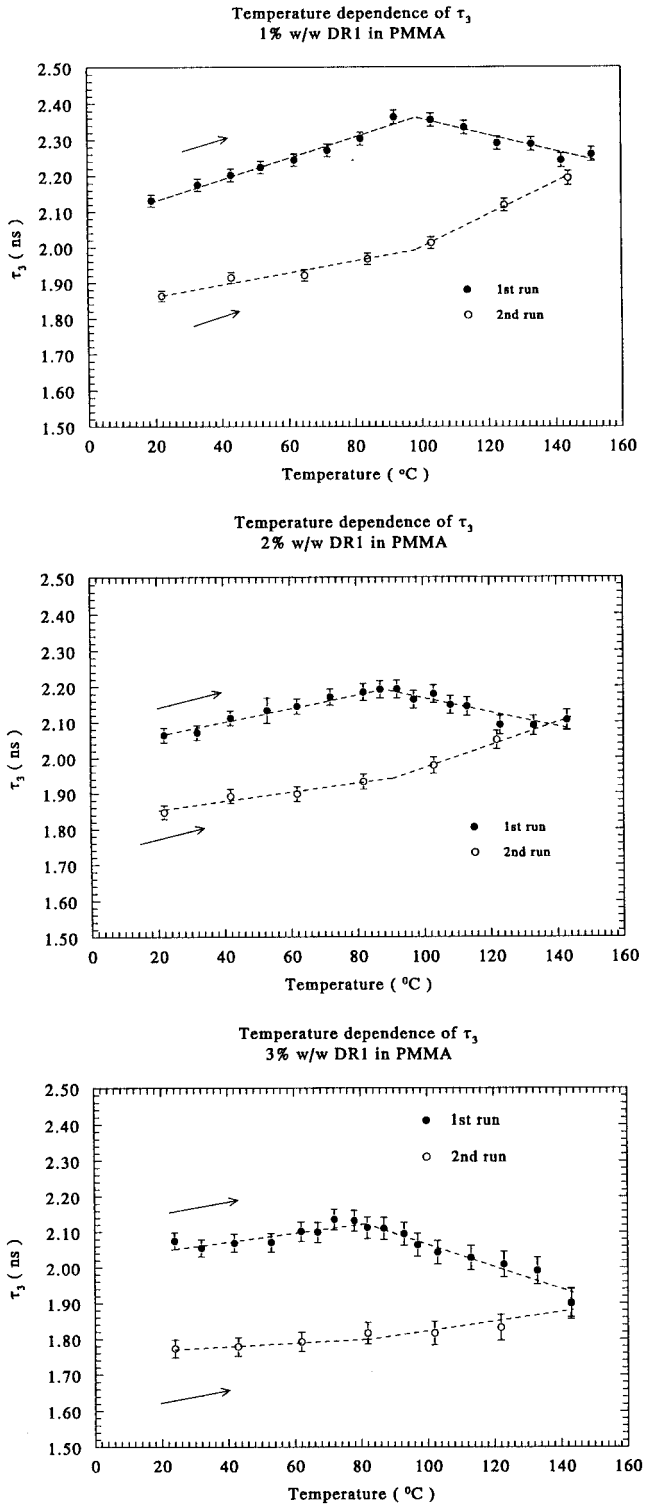

Figure 8. o-Ps lifetime vs temperature in DR1-doped PMMA at different temperatures. Lines were fitted through data in two temperature regions.

3. Ps Reaction with Chromophores. The molecular structure of doped chromophores contains a nitro ($-NO_2$) functional group which is known to be a strong quencher for Ps reactions in solutions.[38] The chemical reaction between a chemical quencher (M) and Ps has been postulated through a Ps complex formation mechanism which can be schematically shown as[38]

$$2\gamma \xleftarrow{\lambda_p} \mathrm{Ps} + \mathrm{M} \underset{k_b}{\overset{k_a}{\rightleftharpoons}} \mathrm{Ps{-}M} \xrightarrow{\lambda_c} 2\gamma \qquad (3)$$

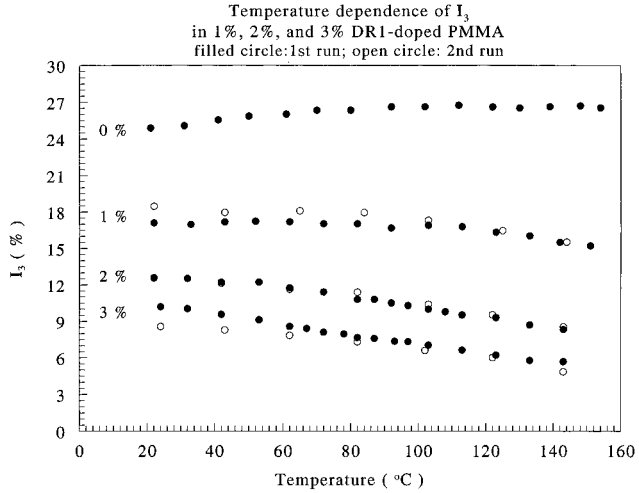

Figure 9. o-Ps intensity vs temperature in DR1-doped PMMA.

where λ_p is the rate constant for Ps annihilation with PMMA polymers (the pick-off annihilation rate), λ_c is the rate constant for Ps annihilation by the Ps/chromophore complex, and k_a and k_b are the rate constants for formation and dissociation of the Ps/molecular complexes. The chemical reaction rate constant between Ps and chromophore molecules can be expressed with the pseudo-first-order kinetics as $k_{Ps} = k_a\lambda_c/(k_b + \lambda_c)$. The k_{Ps} quantity is a measurable quantity from the PAL experiment:

$$\lambda_3 = \lambda_p + k_{Ps}[M] \tag{4}$$

where λ_3 is the reciprocal of the measured o-Ps lifetime (τ_3) at a certain chromophore concentration [M] (in units of mol/L), and k_{Ps} is a measure of chemical reactivity between the Ps and chromophore in the PMMA matrix. In Figure 12, we plot the λ_3 vs concentration of chromophores in PMMA at selected temperatures. Linear relationships support the above postulated Ps complex formation mechanism. The slope of these plots gives k_{Ps} values on the order of $(0.2-1.5) \times 10^9$ M^{-1} s^{-1} for these chromophores in PMMA polymers. These are comparable with dinitrobenzene values in polycarbonate, polystyrene, and polysufones.[39] They are about 1−2 orders of magnitude smaller than the k_{Ps} of these types of molecules in liquids.[40] Lower Ps chemical reactivity in polymers is expected due to the low mobility of doped molecules in polymers compared to liquids.[41]

Because nitroaromatics are strong quenchers for Ps reactions, we invoke reaction kinetics in terms of the Smolouchowski diffusion-controlled equation for k_{Ps} as[40]

$$k_{Ps} = 4\pi(10^{-3})N_0(D_{Ps} + D_M)(r_{Ps} + r_M) \tag{5}$$

where D_{Ps} and D_M (in cm^2/s) are the diffusion coefficients of Ps and chromophores, N_0 is Avogadro's number, and r_{Ps} and r_M are the radii of Ps and M, respectively. Here the Ps radius is approximated by its Bohr radius (0.053 nm), and the chromophore size is taken to be 0.46 nm. Due to the larger size of chromophores and lower molecular mobility compared with Ps, we can neglect chromophore diffusion coefficients in the above equation. The diffusion coefficients of Ps can be simplified from the above equation as[39]

$$D_{Ps} = 4.6 \times 10^9 k_{Ps}/(\pi N_0) \tag{6}$$

With the above equation, we determine the diffusion coefficients of Ps in PMMA as a function of temperature. The results determined by DR1 and DO3 are plotted in Figure 13. The

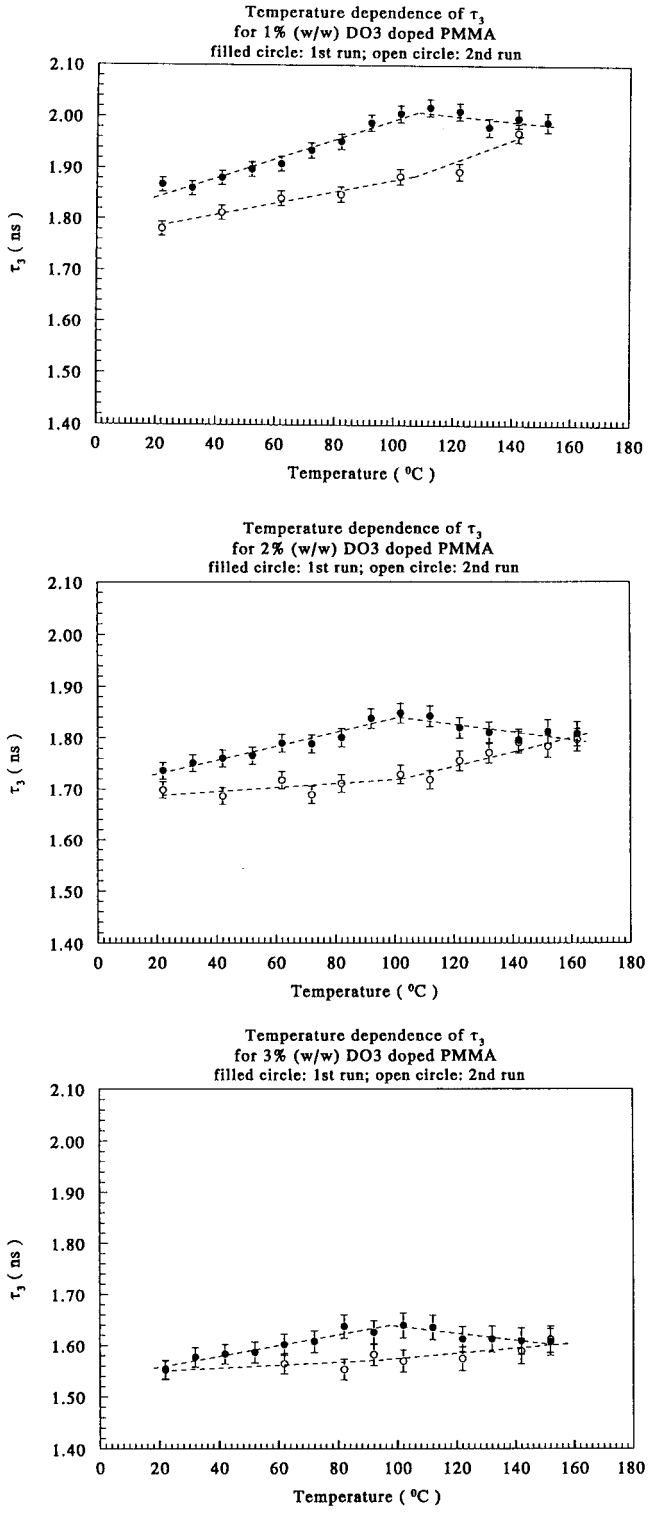

Figure 10. o-Ps lifetime vs temperature in DO3-doped PMMA. Lines were fitted through data in two temperature regions.

values for D_{Ps} at room temperature in PMMA are about 200 times larger than diatomic molecules such as O_2 ($=1.4 \times 10^{-8}$ cm^2/s).[41] The temperature dependence of D_{Ps} then follows the Arrhenius equation from the transition-state theory as described above. The variation of D_{Ps} vs temperature is shown in Figure 13. It is interesting to observe temperature dependence of diffusion coefficients for Ps in polymers opposite to that of positron diffusion in crystalline solids. In perfect solids, positron diffusion is described by the phonon theory, and its temperature dependence is in the form of $D_+ \approx T^{-1/2}$.[42,43] In perfect lattices,

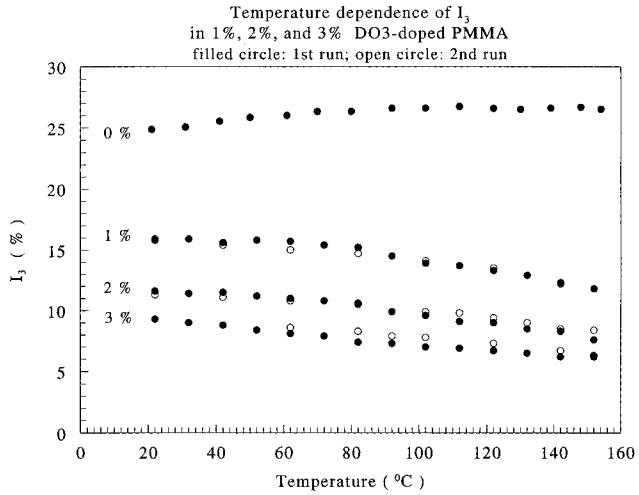

Figure 11. o-Ps intensity vs temperature in DO3-doped PMMA.

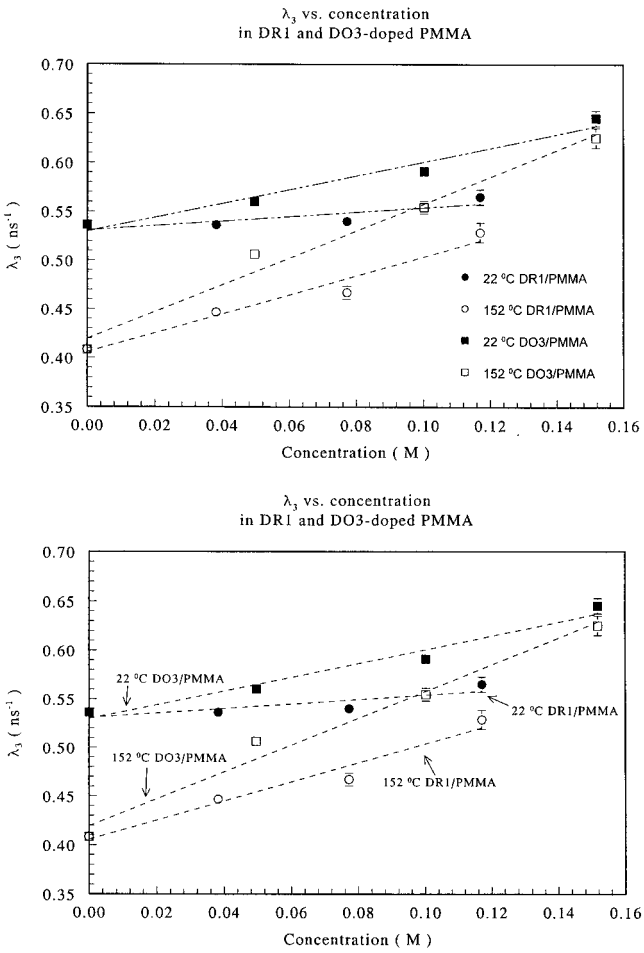

Figure 12. o-Ps annihilation rate ($\lambda_3 = 1/\tau_3$) vs chromophore concentration. The slopes of the fitted line are k_{Ps} according to eq 4.

D_+ decreases as a function of temperature. In polymeric materials that contain a large fraction of defects, the Ps diffusion is described in a thermally active process similar to atomic diffusion in polymeric systems.[44] Furthermore, the positron diffusion coefficient (D_+) in amorphous polymers is estimated from τ_2 data to be on the order of 10^{-3} cm^2/s, which is several orders of magnitude smaller than that in crystalline solids.[45]

The reduction of the o-Ps formation fraction (I_3) due to the presence of chromophore doping is often called the inhibition of Ps formation. Molecules containing a nitro group are known to be good electron scavengers. Doping of chromophores in

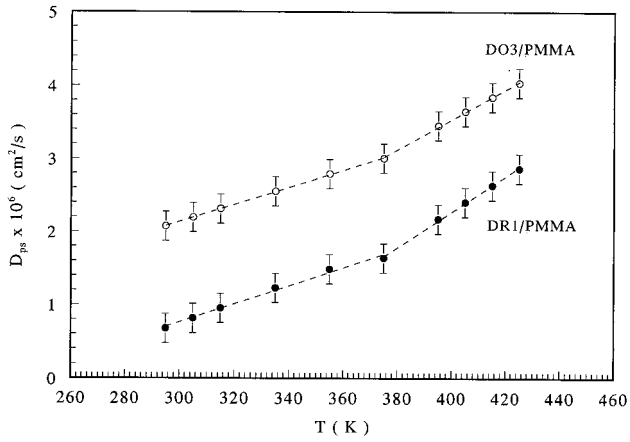

Figure 13. Ps diffusion coefficient vs temperature for DO3- and DR1-doped PMMA systems.

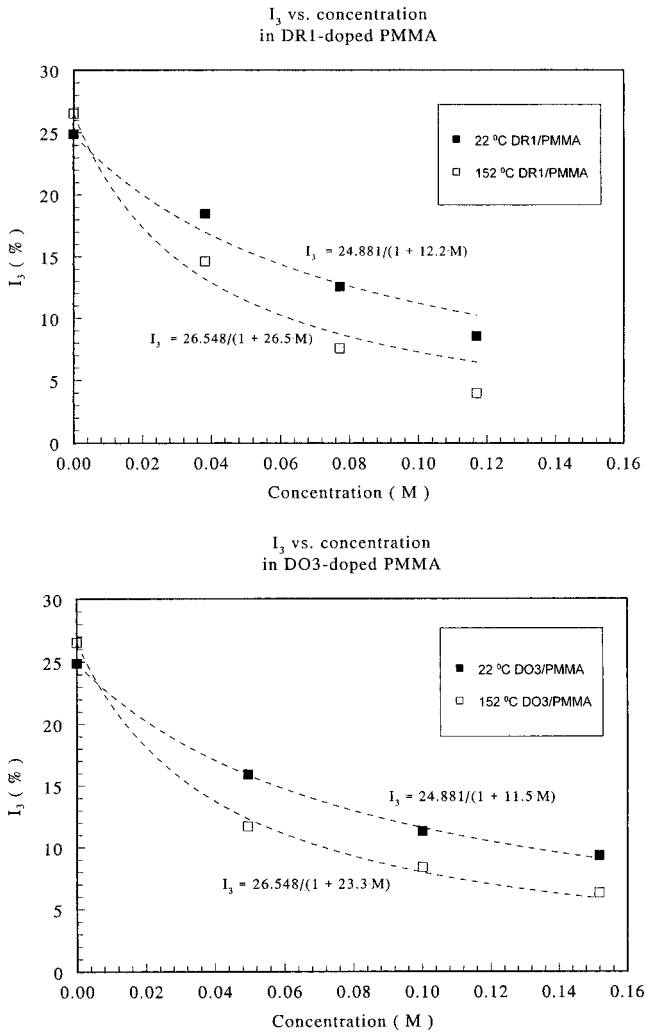

Figure 14. o-Ps intensity vs chromophore concentration. Lines are fitted according to eq 7.

PMMA is expected to reduce the number of electrons available to the positron to form Ps. As shown in Figure 14, I_3 decreases as a function of doping concentration. The variation of I_3 fits nicely into an empirical equation as[40]

$$I_3 = I_o/(1 + K_{inhib}M) \quad (7)$$

where I_0 is the I_3 of PMMA without doping and K_{inhib} is called the Ps inhibition constant. The fitted K_{inhib} at room temperature

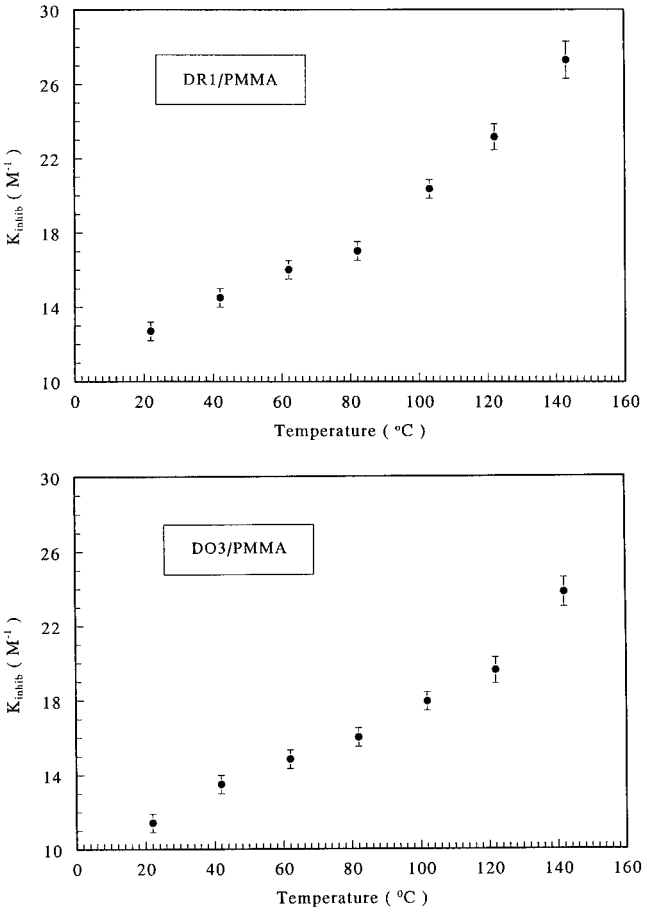

Figure 15. Temperature dependence of Ps inhibition constants in DR1 and DO3/PMMA systems.

is 12.2 and 11.5 ± 0.6 M^{-1} for DR1 and DO3, respectively. In the rubbery state, K_{inhib} is approximately twice (26.5 and 23.3 M^{-1}) that of the glassy state and is comparable to K_{inhib} for nitrobenzene in liquids.[46] The temperature dependence of K_{inhib} is shown in Figure 15, which indicates a thermal process.

4. Temperature Dependence of Doped Systems. The o-Ps lifetime (τ_3) results of temperature dependence in doped chromophores in PMMA systems are shown in Figure 16. The τ_3 results are presented in Figures 9 and 11. As shown in Figures 9 and 11, I_3 decreases as a function of temperature in doped systems. This is opposite to the undoped PMMA results (Figure 4). As discussed in the above section, an increase of I_3 in pure PMMA as a function of temperature indicates an increase in free volume and hole concentration. In doped systems, the variation of I_3 is significantly affected by the scavenging reaction between chromophore molecules and electrons. This so-called "inhibition" effect increases as the temperature increases. Thus, a decrease in o-Ps formation (I_3) is seen as the temperature increases in doped systems (Figures 9 and 11). It is worth mentioning that, in a system which contains a Ps-inhibiting molecule, the fractional free volume described in eq 2 cannot be directly used.

The large temperature dependence of τ_3 as shown in Figure 16 is related to the viscoelasticity of polymers. Each curve shows two regions of variation: one at low temperature and the other at high temperatures. We follow the same interpretation here as with pure PMMA; namely, two slopes intercept at a certain temperature that corresponds to T_g as probed by o-Ps lifetimes. It is obvious that the intercept temperature decreases as a function of chromophore doping. We plot the intercept temperatures in Figure 17 and compare with T_g, determined by

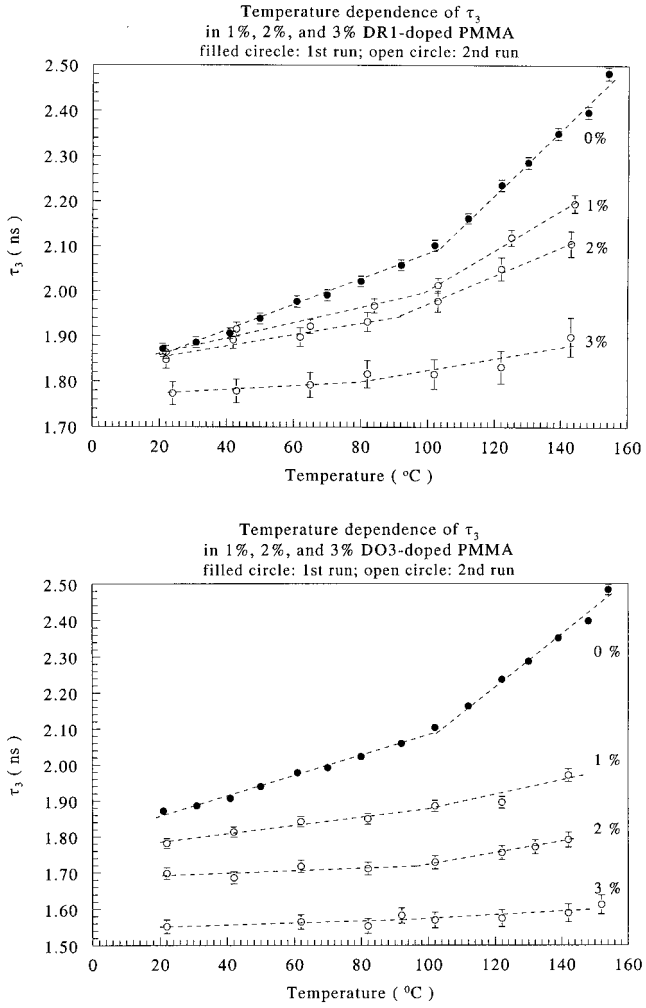

Figure 16. o-Ps lifetime vs temperature for DR1- or DO3-doped PMMA systems. The lines were linearly fitted to low and high temperatures, respectively. The intercept temperature is defined as T_g by PAL.

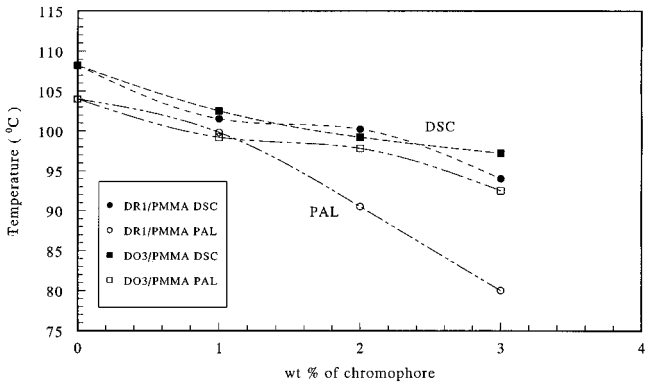

Figure 17. T_g vs wt % of chromophores in PMMA as determined by DSC and PAL methods.

the DSC method. As shown in Figure 17, T_g results are consistent with the DSC results in showing that doping decreases T_g. Also, in all PAL results, T_g determined by o-Ps lifetime is consistently lower than T_g determined by DSC. A decrease of T_g due to doping can be interpreted as resulting from the plasticizing effect of incorporating small molecules into the PMMA matrix.[47,48]

The temperature variation of τ_3, which is the reciprocal of the annihilation rate τ_3, contains important information about the kinetics of Ps in polymers. We calculate the chemical

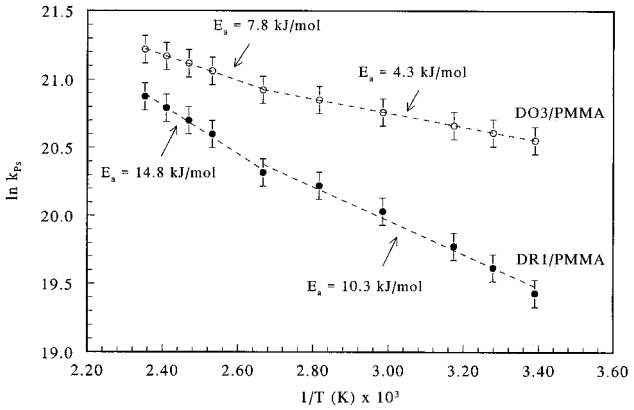

Figure 18. Arrhenius plots of k_{Ps} vs $1/T$ in two chromophores in PMMA systems. The slopes are the activation energy E_a for the Ps reaction with chromophores according to the kinetic scheme shown in eq 3.

reaction rate constants, k_{Ps}, from τ_3 ($1/\lambda_3$) data according to eq 4 and plot the results vs the reciprocal of the temperature in Figure 18. According to the transition-state theory for chemical reactions, the Ps reaction is expressed by the Arrhenius equation as[38,40]

$$k_{Ps} = A \exp(-E_a/RT) \tag{8}$$

where E_a is the activation energy for Ps reacting with chromophore molecules in a PMMA matrix according to the kinetic scheme of eq 3, and A is the preexponential factor. We fit the data with a single slope as well as with two slopes and consistently find that two slopes give a significantly better fit. The temperature where the slope changes is near T_g of the doped systems. We therefore report here two activation energies: one for low temperatures (glassy state) and the other for high temperatures (rubbery state). E_a values for DR1 above and below T_g are 14.8 ± 1.0 and 10.3 ± 1.0 kJ/mol, respectively; E_a values for DO3 above and below T_g are 7.8 ± 1.0 and 4.3 ± 1.0 kJ/mol, respectively. It is interesting to observe a smaller E_a for a smaller chromophore (DO3) than for a larger molecule (DR1). These E_a are relatively small compared to the activation energies for common chemical reactions. This is indicative of the diffusion-controlled mechanism for Ps reactions with chromophores in polymeric materials. E_a results in PMMA are comparable to those values for nitrobenzene in organic solvents.[40]

IV. Conclusion

We report a temperature study of positron annihilation in two chromophores, DR1 and DO3, in PMMA polymers. The o-Ps lifetime variations are interpreted in terms of free volume and hole properties and Ps chemical kinetics. Doping of chromophores in PMMA is found to decrease T_g due to the plasticizing effect. The kinetics of Ps reactions with chromophores are described by a Ps molecular complex formation mechanism. Ps diffusion coefficients are found to increase with temperature. Applications of PAL to probe the local free volumes and related nonlinear optical properties appear promising in the future.

Acknowledgment. This work has been supported by a grant from the Air Force Office of Scientific Research (AFOSR) of the U.S. (F49620-97-1-0162). Fruitful discussions with Prof. T. C. Sandreczki are acknowledged.

References and Notes

(1) Dalton, L. R.; Harper, A. W.; Ghosn, R.; Steier, W. H.; Ziari, M.; Fetterman, H.; Shi, Y.; Mustacich, R. V.; Jen, A. K.-Y.; Shea, K. *Chem. Mater.* **1995**, *7*, 1060.

(2) Bosshard, C.; Sutter, K.; Prete, P.; Hullinger, J.; Florsheimer, M.; Kaatz, P.; Gutter, In *Organic Nonlinear Optical Materials: Advances in Nonlinear Optics*; Gordon & Breach Publishers: Postfach, Switzerland, 1995; Vol. 1, Chapter 6.

(3) Marder, S. R.; Perry, J. W. *Science* **1994,** *263*, 1706.

(4) Hampsch, H. L.; Yang, J.; Wong, G. K.; Torkelson, J. M. *Macromolecules* **1990**, *23*, 3640.

(5) Man, H. T.; Yoon, H. N. *Adv. Mater.* **1992**, *4*, 159.

(6) Singer, K. D.; King, L. A. *J. Appl. Phys.* **1991**, *70*, 3251.

(7) Stahelin, M.; Walsh, C. A.; Burland, D. M.; Miller, R. D.; Twieg, R. J.; Volksen, W. *J. Appl. Phys.* **1993**, *73*, 8471.

(8) Hampsch, H. L.; Yang, J.; Wong, G. K.; Torkelson, J. M. *Polym. Commun.* **1989**, *30*, 40.

(9) Walsh, C. A.; Burland, D. M.; Lee, V. Y.; Miller, R. D.; Smith, B. A.; Twieg, R. J.; Volksen, W. *Macromolecules* **1993**, *26*, 3720.

(10) Kalachandra, S.; Turner, D. T. *J. Polym. Sci. B: Polym. Phys.* **1987**, *25*, 1971.

(11) Bauer-Gugonea, S.; Berhard-Multhaupt, R. *IEEE Trans. Dielectr. Electr. Insul.* **1996**, *3*, 677.

(12) Madani, M. M.; Miron, R. R.; Granata, R. D. *J. Coat. Technol.* **1997**, *69*, 45.

(13) Uedono, A.; Kawano, T.; Tanigawa, T.; Ban, M.; Kyoto, H.; Uozumi, T. *J. Polym. Sci. B: Polym. Phys.* **1997**, *35*, 1601.

(14) Wastlund, C.; Maurer, F. H. J. *Macromolecules* **1997**, *30*, 5870.

(15) Chang, G. W.; Jamieson, A. M.; Yu, Z. B.; MacGervey, J. D. *J. Appl. Polym. Sci.* **1997**, *63*, 483.

(16) Hristov, H. A.; Bolam, B.; Yee, A. F.; Xie, L.; Gidley, D. W. *Macromolecules* **1996**, *29*, 8507.

(17) Hill, A. J.; Zipper, M. D.; Tant, M. R.; Atock, G. M.; Jordan, T. C.; Sultz, A. R. *J. Phys.: Condens. Matter* **1996**, *8*, 3811.

(18) Borek, J.; Osoba, W. *J. Polym. Sci. B: Polym. Phys.* **1996**, *34*, 1903.

(19) Hong, X.; Jean, Y. C.; Yang, H.; Jordan, S. S.; Koros, W. J. *Macromolecules* **1996**, *29*, 7859.

(20) Jean, Y. C. *Microchem. J.* **1990**, *42*, 72.

(21) PATFIT package, 1989; purchased from Riso National Laboratory, Denmark.

(22) Provencher, S. W. *Comput. Phys. Commun.* **1982**, *27*, 213.

(23) Shukla, A.; Peter, M.; Hoffmann, L. *Nucl. Instrum. Methods* , **1993**, *335*, 310.

(24) Cao, H.; Dai, G. H.; Yuan, J. P.; Jean, Y. C. *Mater. Sci. Forum* **1997**, *255*−*257*, 742.

(25) Tao, S. J. *J. Chem. Phys.* **1972**, *56*, 5499.

(26) Eldrup, M.; Lightbody, D.; Sherwood, J. N. *Chem. Phys.* **1981**, *63*, 51.

(27) Nakanishi, H.; Wang, S. J.; Jean, Y. C. In *Positron Annihilation Studies of Fluids*; Sharma, S. C., Ed.; World Scientific: Singapore, 1988; p 292.

(28) Wang, Y. Y.; Nakanishi, H.; Jean, Y. C.; Sandreczki, T. C. *J. Polym. Sci. B* **1990**, *28*, 1431.

(29) Mahotra, B. D.; Pethrick, R. A. *Macromolecule*, **1983**, *16*, 1175.

(30) Bartos, J. *Colloid Polym. Sci.* **1996**, *14*, 274.

(31) Hasan, O. A.; Boyce, M. C.; Li, X. S.; Berko, S. *J. Polym. Sci. B: Polym. Phys.* **1993**, *31*, 185.

(32) Jean, Y. C.; Sandreczki, T. C.; Ames, D. P. *J. Polym. Sci. Phys.* **1986**, *24*, 1247.

(33) Yang, L.; Hiristov, H. A.; Yee, A. F.; Gidley, D. W.; Halary, J. L.; Monnerie, C. *Polymer* **1995**, *36*, 3997.

(34) Xie, L.; Gidley, D. W.; Hristov, H. A.; Yee, A. F. *J. Polym. Sci. B: Polym. Phys.* **1995**, *33*, 77.

(35) Sandreczki, T. C.; Hong, X.; Jean, Y. C. *Macromolecules* **1996**, *29*, 4015.

(36) Jean, Y. C. In *Positron Spectroscopy of Solids*; Dupasquier, A., Mills, Jr., A. P., Eds.; IOS: Ohmsha, 1995; p 563.

(37) Duplatre, O. E.; Billard, I.; Abbe, J. ch. *Chem. Phys.* **1994**, *184*, 371.

(38) Madia, W. J.; Nichols, A. L.; Ache, H. *J. Am. Chem. Soc.* **1975**, *97*, 5041.

(39) Hirata, K.; Kobauashi, Y.; Ujihira, Y. *J. Chem. Soc., Faraday Trans.* **1996**, *92*, 985.

(40) For example, see: Nakanishi, H.; Jean, Y. C. In *Positron and Positronium Chemistry*; Schrader, D. M., Jean, Y. C., Eds.; Elsevier Science: Amsterdam, 1988; Chapter 5.

(41) Barker, Jr., R. E. *J. Polym. Sci.* **1962**, *58*, 553.

(42) Bergersen, B.; Pajanne, E.; Kubica, P.; Stott, M. J.; Hodges, C. H. *Solid. State Commun.* **1974**, *15*, 1377.

(43) Lynn, K. G. In *Positron Studies of Solids, Surfaces, and Atoms*; Mills, Jr., A. P., Crane, W. S., Canter, K. F., Eds.; World Scientific: Singapore, 1986; p 70.
(44) Willecke, R.; Faupel, F. *J. Polym. Sci. B: Polym. Phys*. **1997**, *35*, 1043.
(45) Brandt, W. *Appl. Phys. A* **1974**, *5*, 1.
(46) Byakov, V. M.; Grafutin, V. I.; Koldaeva, O. V.; Minaichev, E. V. *J. Phys. Chem.* **1980**, *84*, 1867.
(47) Bolink, H. J.; Krasnikov, V. V.; Malliaras, G. G.; Hadziioannou, L. *J. Phys. Chem.* **1996**, *100*, 16356.
(48) Wisnudel, M. B.; Torkelson, J. M. *J. Polym. Sci. B: Polym. Phys.* **1996**, *34*, 2999.